Development 125, 4655-4667 (1998)
Printed in Great Britain © The Company of Biologists Limited 1998
DEV3878

Early development of the zebrafish pronephros and analysis of mutations affecting pronephric function

Iain A. Drummond[1,§], Arindam Majumdar[1], Hartmut Hentschel[3], Marlies Elger[4], Lila Solnica-Krezel[2,‡], Alexander F. Schier[2,‡], Stephan C. F. Neuhauss[2,‡], Derek L. Stemple[2,‡], Fried Zwartkruis[2,‡], Zehava Rangini[2,‡], Wolfgang Driever[2,*] and Mark C. Fishman[2]

[1]Renal Unit, Massachusetts General Hospital, 149 13th street, Charlestown MA 02129, USA
[2]Cardiovascular Research Center, Massachusetts General Hospital, 149 13th street, Charlestown MA 02129, USA
[3]Max Planck Institut für Molekulare Physiologie, MPI Dortmund, Postfach10 26 64, 44026 Dortmund, Germany
[4]Institut für Anatomie und Zellbilogie, Universitåt Heidelberg, 69120 Heidelberg, Germany
*Present address: Department of Developmental Biology, Institute Biology 1, University of Freiburg, Hauptstrasse 1, D-79104 Freiburg, Germany
‡For current addresses refer to the ZFIN database (URL: http://zfish.uoregon.edu/ZFIN/)
§Author for correspondence (e-mail: idrummon@receptor.mgh.harvard.edu)

Accepted 18 September; published on WWW 9 November 1998

SUMMARY

The zebrafish pronephric kidney provides a simplified model of nephron development and epithelial cell differentiation which is amenable to genetic analysis. The pronephros consists of two nephrons with fused glomeruli and paired pronephric tubules and ducts. Nephron formation occurs after the differentiation of the pronephric duct with both the glomeruli and tubules being derived from a nephron primordium. Fluorescent dextran injection experiments demonstrate that vascularization of the zebrafish pronephros and the onset of glomerular filtration occurs between 40 and 48 hpf. We isolated fifteen recessive mutations that affect development of the pronephros. All have visible cysts in place of the pronephric tubule at 2-2.5 days of development. Mutants were grouped in three classes: (1) a group of twelve mutants with defects in body axis curvature and manifesting the most rapid and severe cyst formation involving the glomerulus, tubule and duct, (2) the *fleer* mutation with distended glomerular capillary loops and cystic tubules, and (3) the mutation *pao pao tang* with a normal glomerulus and cysts limited to the pronephric tubules. *double bubble* was analyzed as a representative of mutations that perturb the entire length of the pronephros and body axis curvature. Cyst formation begins in the glomerulus at 40 hpf at the time when glomerular filtration is established suggesting a defect associated with the onset of pronephric function. Basolateral membrane protein targeting in the pronephric duct epithelial cells is also severely affected, suggesting a failure in terminal epithelial cell differentiation and alterations in electrolyte transport. These studies reveal the similarity of normal pronephric development to kidney organogenesis in all vertebrates and allow for a genetic dissection of genes needed to establish the earliest renal function.

Key words: Zebrafish, Pronephros, Kidney, Nephron, *fleer*, *pao pao tang*, *double bubble*

INTRODUCTION

The pronephros is the first kidney to form during development in vertebrates (Saxén, 1987) and in fish and amphibians remains the primary blood filtration and osmoregulatory organ in free-swimming larvae (Howland, 1921; Tytler, 1988; Tytler et al., 1996; Vize et al., 1997). In comparison to the mesonephric kidney, which develops later as juvenile fish mature into adults (Agarwal and John, 1988), and the metanephric kidney found in other vertebrates, the teleost pronephros is a relatively simple organ. It is composed of a pair of nephrons with two glomeruli fused at the midline, pronephric tubules connecting directly to the glomeruli via a neck segment and paired bilateral pronephric ducts which convey the altered blood filtrate outside the animal (Tytler, 1988; Tytler et al., 1996). The teleost pronephros shares many essential features with the amphibian pronephros including its derivation from mesoderm associated with the coelom and the derivation of the glomerular blood supply from the medial dorsal aorta (Armstrong, 1932; Vize et al., 1997). However, unlike the pronephros of amphibians, which have an external glomus and tubules with nephrostomes open to the coelom (Howland, 1921; Goodrich, 1930; Jaffe, 1954; Vize et al., 1997), the mature teleost pronephros has no connection to the body cavity and instead functions as a closed system (Goodrich, 1930; Armstrong, 1932; Tytler, 1988). Although the overall structure of the zebrafish pronephros is distinctive, processes of tubular and glomerular differentiation are similar

to kidneys in higher vertebrates, as evidenced by the cellular architecture of the pronephric glomerulus and in the specialized transport functions of pronephric tubular epithelial cells (Tytler, 1988). These features make the zebrafish pronephros a simple and accessible system to study the differentiation of renal cell types and the genesis of nephron form and function.

In zebrafish, the presumptive pronephric primordium is first evident during early somitogenesis as a mass of intermediate mesoderm that lies under the second and third somite (Kimmel et al., 1995). From this position on both sides of the embryo, pronephric ducts grow caudally under the somites. By 24 hours, the ducts are patent epithelial tubules that have fused at their posterior and exit the embryo at the position of the anus (Kimmel et al., 1995). Much less is known about the development of the pronephric nephron itself. Morphological studies in other fish species suggest that nephron primordia are present at the rostral tips of the pronephric ducts and give rise to the pronephric glomeruli and tubules (Armstrong, 1932; Newstead and Ford, 1960; Agarwal and John, 1988; Tytler et al., 1996). However, the intermediate steps in the formation of the pronephros, the timing of onset of pronephric function and the identity of genes required for these processes are currently unknown.

Largely as a result of gene-targeting experiments in mice, a variety of genes have been shown to play essential roles in the early steps of metanephric kidney development. These genes encode secreted molecules such as Wnt4, PDGF, BMP7 and GDNF (Leveen et al., 1994; Soriano, 1994; Stark et al., 1994; Dudley et al., 1995; Moore et al., 1996; Pichel et al., 1996; Sanchez et al., 1996), transcription factors Wt1, Pax2, BF-2, Emx2 and Lim-1 (Kreidberg et al., 1993; Shawlot and Behringer, 1995; Torres et al., 1995; Hatini et al., 1996; Miyamoto et al., 1997), the cell-surface receptor c-ret (Schuchardt et al., 1994), and matrix receptors, integrin alpha3 and alpha8 (Kreidberg et al., 1996; Muller et al., 1997). In zebrafish, the no isthmus (*noi*) mutation has revealed the importance of *pax2.1* expression for the maintenance of the pronephric duct epithelia (Brand et al., 1996; Chen et al., 1996). However, with the exception of Lim-1, which may be essential for the development of the entire urogenital system (Shawlot and Behringer, 1995), no other genes have been demonstrated to be essential for the development of the pronephros. Here we characterize the early steps in zebrafish pronephric nephron formation and establish the stage when glomerular filtration begins. In addition, we describe and categorize a set of mutations that appear to perturb the earliest functions of the pronephros, giving rise to cysts as well as causing a loss of epithelial polarity in the pronephric duct. We find that cyst development coincides with the development of the glomerulus and the onset of glomerular function.

MATERIALS AND METHODS

Genetic analysis

Mutagenesis was performed on G_0 males with ENU and mutants were identified in sibling crosses of F_2 progeny as described previously (Driever et al., 1996). Characteristic mutant phenotypes have been observed in at least three outcrosses for each mutant. Mutant lines were maintained in an AB or AB/Tübingen hybrid genetic background. Mutant embryos for phenotypic analysis were produced by sibling mating. Mutants were grouped by the presence of a straight or curved body axis and subjected to complementation analysis within each group. Complementation group assignment was confirmed by at least two crosses producing >50 embryos each. Mutations with grossly similar morphology to the cyst mutants described here have also been isolated in the large-scale mutagenesis screen carried out in Tübingen (Brand et al., 1996; Chen et al., 1996; Haffter et al., 1996); however, no detailed information of their phenotype has been presented.

Phenotypic analysis

Embryos were maintained at 28°C in egg water (Westerfield, 1994). For histological analysis embryos were fixed in BT fix (4% paraformaldehyde /4% sucrose/0.1M sodium phosphate (pH 7.3)/0.15 mM $CaCl_2$; (Westerfield, 1994)), embedded in JB-4 resin (Polysciences Inc.) and sectioned at 3-5 μm. Slides were stained in methylene blue/azure II (Humphrey and Pittman, 1974). At least 10 mutant embryos were examined for each time point. For electron microscopy, embryos were fixed and sectioned as previously described (Hentschel, 1991). In situ hybridization was carried out as described (Oxtoby and Jowett, 1993) using probes to pax2.1 (Krauss et al., 1991) and the zebrafish *wt1* homolog (F. Serluca et al. unpublished results). Stained embryos were embedded in JB-4 and sectioned. Whole-mount immunocytochemistry was performed on embryos fixed in methanol:DMSO (80:20) as described (Dent et al., 1989; Westerfield, 1994). The monoclonal antibody alpha 6F, raised against the chicken alpha1 subunit of the Na^+/K^+ ATPase (Takeyasu et al., 1988), was obtained from the Developmental Studies Hybridoma Bank and used in conjunction with Cy3- or HRP-labeled secondary antibodies. Whole-mount embryos were embedded in JB-4, sectioned at 4 μm and mounted in Gel-mount (Biomeda Inc.). Endogenous alkaline phosphatase activity was detected by incubating JB-4 tissue sections on slides directly in alkaline phosphatase substrate (0.34 mg/ml nitroblue tetrazolium, 0.18 mg/ml X-phosphate, 100 mM Tris pH 9.5, 100 mM NaCl, 50 mM $MgCl_2$).

Dye filtration experiments

A 1% solution of lysine-fixable rhodamine dextran (10,000 M_r; Molecular Probes) was prepared in PBS and injected into the sinus venosus of immobilized embryos using glass micropipets. Prior to injection, embryos were anaesthetized using a 0.2 mg/ml tricaine solution in egg water (Westerfield, 1994). After 5 minutes, the dye had perfused the circulatory system and the embryos were fixed, embedded in JB-4, sectioned at 3 μm and mounted in Gel-mount.

All microscopy was performed on a Zeiss Axioplan. Photographic slides were scanned and composite figures were prepared using Adobe photoshop software and printed on a Tektronics Phaser 440 printer.

RESULTS

The zebrafish pronephros

The zebrafish pronephros in hatched 3-day-old larvae consists of a glomerulus, pronephric tubules and paired pronephric ducts. The glomerulus and tubules lie below the third somite and just caudal to the pectoral fins (Fig. 1A). The complete system of paired pronephric tubules and ducts can be visualized in a 3 day larva with the monoclonal antibody alpha6F raised against the chick Na^+/K^+ ATPase (Takeyasu et al., 1988) (Fig. 1B). This strong staining in these epithelia is consistent with an osmoregulatory function for the pronephros in freshwater fish. The anterior half of the pronephric ducts as well as the pronephric tubules can also be visualized in 3 day larvae with the monoclonal antibody 3G8 (Vize et al., 1995)

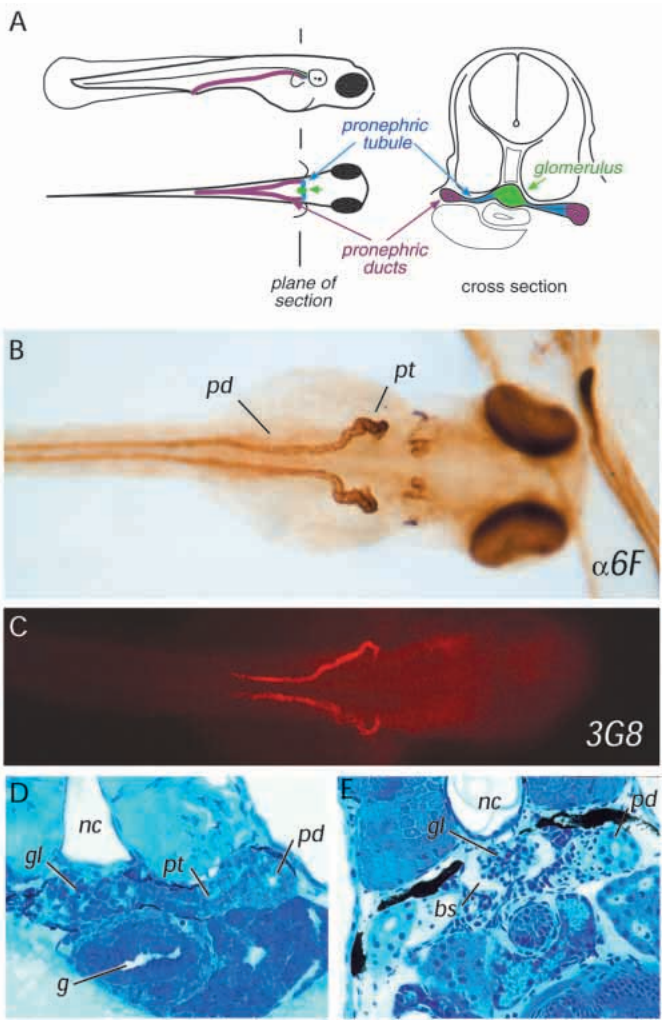

Fig. 1. The zebrafish pronephros. (A) Diagram of the three elements of the larval pronephros at 72 hpf showing the position of glomerulus under the notochord, the pronephric tubules extending laterally to connect with the pronephric ducts which serve the function of the collecting system. (B) Horseradish peroxidase whole-mount immunostaining of a 84 h embryo with anti-Na^+/K^+-ATPase alpha subunit monoclonal antibody (α6F;) shows the overall anatomy of the pronephric ducts (*pd*) and pronephric tubules (*pt*), which become progressively convoluted. The glomerulus is unstained at the embryo midline. (C) The monoclonal antibody 3G8 stains the anterior half of the pronephric ducts as well as the lateral part of the pronephric tubules. (D) Cross section of a 72 h embryo showing that the glomerulus (*gl*), the pronephric tubule (*pt*) and the pronephric duct (*pd*) are fully formed between the gut (*g*) and the notochord (*nc*). (E) In a 6.5-day-old larva, Bowman's space (*bs*) is clearly evident in the glomerulus (*gl*).

(Fig. 1C). In histological sections, a glomerular mass is evident directly ventral to the notochord and the dorsal aorta (Fig. 1D). The pronephric tubules at this stage run laterally from the glomerulus and connect to the pronephric ducts (Fig. 1D). In 6-day-old larvae, a clear Bowman's space is evident surrounding the glomerular tuft (Fig. 1E) and the pronephric tubules become progressively more convoluted (not shown). The pronephros persists in this position for at least 1 month after hatching (data not shown).

Early development of the pronephros

Previous studies have established that the pronephric ducts are fully formed and patent to the exterior by 24 hours postfertilization (hpf) (Kimmel et al., 1995). However, the formation of the pronephric tubules and glomeruli in zebrafish has not been described. Guided by the position of the mature pronephric nephron, we examined the cellular structures medial to the anterior tips of the pronephric ducts at various time points in order to define the stages of nephron formation. At 24 hpf a nephron primordium is present ventral to the third somite (Fig. 2A,B). The primordium at this stage appears as an infolding of the coelomic lining and a clear opening to the coelom is apparent (Fig. 2A). This opening to the coelom could be considered the equivalent of a nephrostome observed in other fish species and in mature amphibian pronephroi (Goodrich, 1930; Armstrong, 1932). In sagittal view, the pronephric nephron primordium appears as a disk-shaped group of cells with no morphologically distinct tubules or glomeruli (Fig. 2B). The anterior tips of the pronephric ducts lie directly adjacent to the lateral edges of the nephron primordia (Fig. 2B). By 32-33 hpf, the separation of the nephron primordium from the coelom is complete and it appears as a distinct and separate group of cells with no connection to the body cavity (Fig. 2C,D). In cross section (Fig. 2C), a central lumen or nephrocoele is seen and the nephron primordium consists of a flattened vesicle of cells. Sagittal sections at 32-33 hpf reveal the first signs of pronephric nephron morphogenesis (Fig. 2D). The primordium at this stage appears to be partitioned into lateral and medial domains in the regions of the future tubules and glomeruli, respectively (Fig. 2D). At 40 hpf, a clear morphological distinction is apparent between midline cells and cells lying more laterally, adjacent to the anterior tip of the pronephric duct (Fig. 2E). In cross section, midline cells appear to be enclosed by a basement membrane or capsule, while lateral cells are beginning to take on the appearance of the pronephric tubule (Fig. 2E; see below). The morphological distinction between tubule and glomerulus is also apparent in sagittal section where paired oval masses of presumptive glomerular cells are observed at the midline and pronephric tubules are seen emanating from the lateral aspect of the forming glomerulus (Fig. 2F). Longitudinal sections through the midline show the intimate contact between the presumptive glomerulus and the overlying dorsal aorta (Fig. 2G). By 50 hpf, the medial surfaces of the two glomerular primordia have fused at the midline and the pronephric tubule can be seen in sagittal view to arc over laterally where it is connected to the pronephric ducts by a patent lumen (Fig. 2H). The direct connection between the tubule and glomerulus can be seen in cross sections at 60 hpf (Fig. 2I) and also later at 72 hpf (Fig. 2J). This histological analysis suggests that after the separation of the paired nephron primordia from the coelom, each pronephric nephron differentiates as an integrated group of cells to form a closed pronephric system with the bilaterally paired tubules directly connected to midline fused glomeruli.

Expression of *pax2.1* and *wt1* in the forming pronephros

The *pax2* and *wt1* genes have been shown to be essential regulators of nephrogenesis in higher vertebrates (Kreidberg et al., 1993; Torres et al., 1995). These genes and their expression

patterns are also conserved amphibians (Carroll and Vize, 1996; Semba et al., 1996; Heller and Brandli, 1997). In the mouse metanephros, *pax2* is expressed in pronephric duct as well as in the forming kidney tubules and, in the *Xenopus* pronephros, expression of *pax2* can be similarly observed in the pronephric duct and forming pronephric tubules (Dressler and Douglass, 1992; Puschel et al., 1992; Heller and Brandli, 1997). In the metanephros, *wt1* is expressed at a low level in the nephrogenic mesenchyme then becomes upregulated in the condensed mesenchyme/renal vesicle stage (Buckler et al., 1991; Armstrong et al., 1993). In the maturing S-shaped body stage of nephrogenesis, *wt1* expression becomes restricted to a group of cells destined to become podocytes. Expression is also maintained at a lower level in mature podocytes. Expression of *wt1* has also been observed in the developing amphibian pronephric glomus (Carroll and Vize, 1996; Semba et al., 1996). We have used the zebrafish homologs of *pax2* and *wt1* to assess the progress of pronephric nephron differentiation.

The early stages of *pax2.1* (formerly *pax[zf-b]*, Krauss et al., 1991, now designated *pax2.1*, Pfeffer et al., 1998) expression in the intermediate mesoderm and other tissues have been described and, by 24 hpf, expression is seen primarily in the anterior portion of the pronephric duct (Fig. 3A; Krauss et al., 1991; Puschel et al., 1992). In the early stages of nephron morphogenesis (30-33 hpf), a new domain of *pax2.1* expression can be seen anterior and medial to the tips of the pronephric ducts in the position of the future pronephric tubules (Fig. 3B). The *pax2.1* staining does not extend to include the entire nephron primordium. This can be seen clearly in cross section where *pax2.1* expression in the primordium is restricted to cells in the lateral halves of the primordia (Fig. 3C). Soon after this stage, *pax2.1* is downregulated but continues to be expressed at a low level in the tubules and ducts (data not shown). *wt1* is first expressed in intermediate mesoderm at the level of somites 1-3 and, by 24 hpf, becomes concentrated in the forming nephron primordium (Fig. 3D) ventral to somite three. At 33 hpf *wt1* is expressed uniformly throughout the nephron primordium (Fig. 3E) but, by 36 hpf, expression becomes restricted to cells lying under the notochord in the position of the future glomerulus (Fig. 3F). Lateral pronephric tubule cells are negative for *wt1* expression (Fig. 3F). The data suggest that the mediolateral

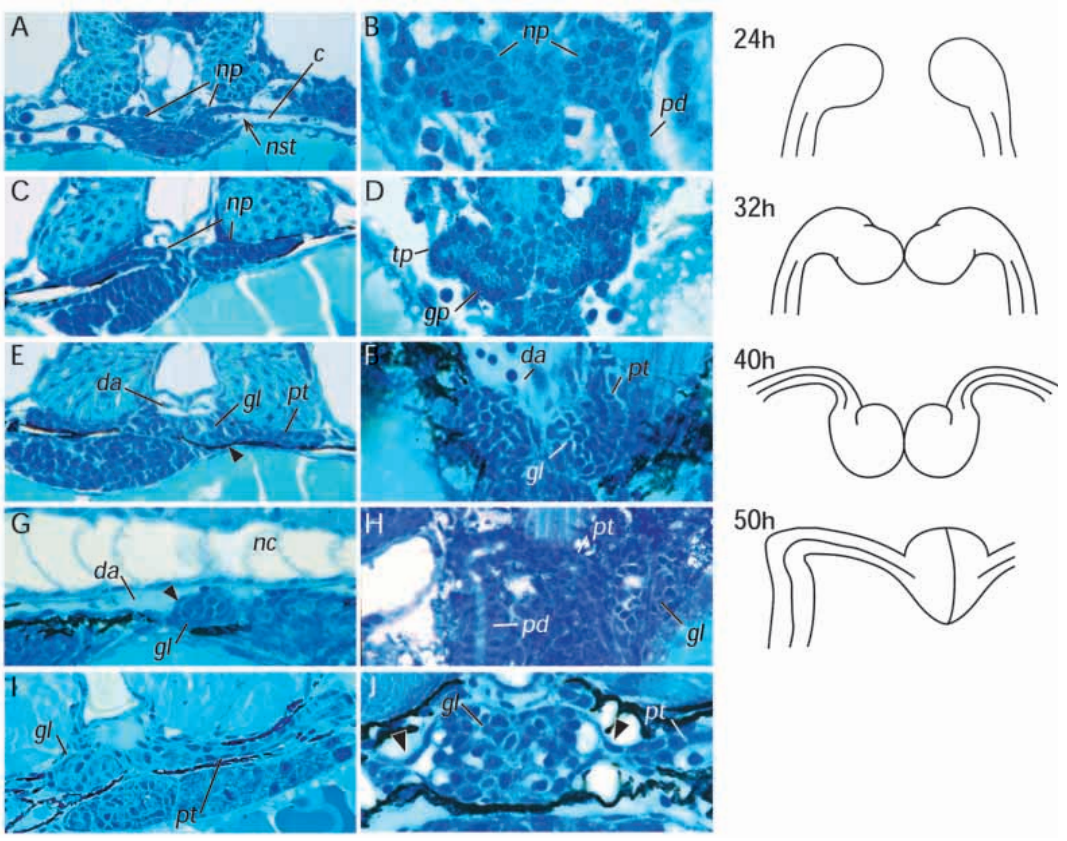

Fig. 2. Pronephric nephron development. (A) Cross section of wild-type pronephroi at 24 hpf shows the forming nephron primordium (*np*) as an invagination of the coelomic lining. The lumen of the nephron precursor, or nephrocoel, is still connected to the coelom (*c*) at this stage by a transient nephrostome *(nst;* arrow*)*. (B) Sagittal section at 24 h shows the anterior pronephric duct (*pd*) abutting on the lateral aspect of the nephron primordium (*np*). C) At 32 h, the nephron primordium is closed off from the coelom and appears as a double-layered sac of cells with a central lumen. (D) A sagittal view at 32 h reveals early stages of nephron morphogenesis with lateralmost cells in the position of future tubules (tubule primordium; *tp*) becoming distinct from medial cells in the position of the future glomerulus (glomerular primordium; *gp*). (E) By 40 h, the nephron primordium has become partitioned into a glomerular domain medially directly under the dorsal aorta (*da*) and tubule domains laterally with a distinct basement membrane surrounding the developing glomerulus (arrow). Pigment cells envelope the pronephros at this stage. (F) A sagittal view of the 40 h pronephric nephron shows the medial paired glomeruli (*gl*) with the pronephric tubules (*pt*) fused to their posterior side. *da*, dorsal aorta. (G) Longitudinal sections through the forming glomerulus (*gl*) at 40 h show its position below the notochord (*nc*) and its intimate association with the dorsal aorta (*da*) and cells (arrow), which surround the forming glomerular basement membrane. (H) Sagittal view of the pronephros at 50 h with the glomeruli (*gl*) fused at the midline and the pronephric tubule (*pt*) arcing over to connect to the pronephric duct (*pd*). (I) The pronephros at 2.5 days postfertilization shows paired glomeruli (*gl*) ventral to the aorta and pronephric tubules (*pt*) connecting laterally to the pronephric ducts. (J) By 3 days, nephron formation is essentially complete and the direct connection between Bowman's space and the lumen of the pronephric tubules is evident (arrows). On the right are schematized versions of the micrographs in B, D, F and H, derived from serial sections, illustrating the morphological transitions that occur during pronephric nephron morphogenesis. In all cross sections, the top of the figure is dorsal and in all sagittal sections the top of the figure is anterior.

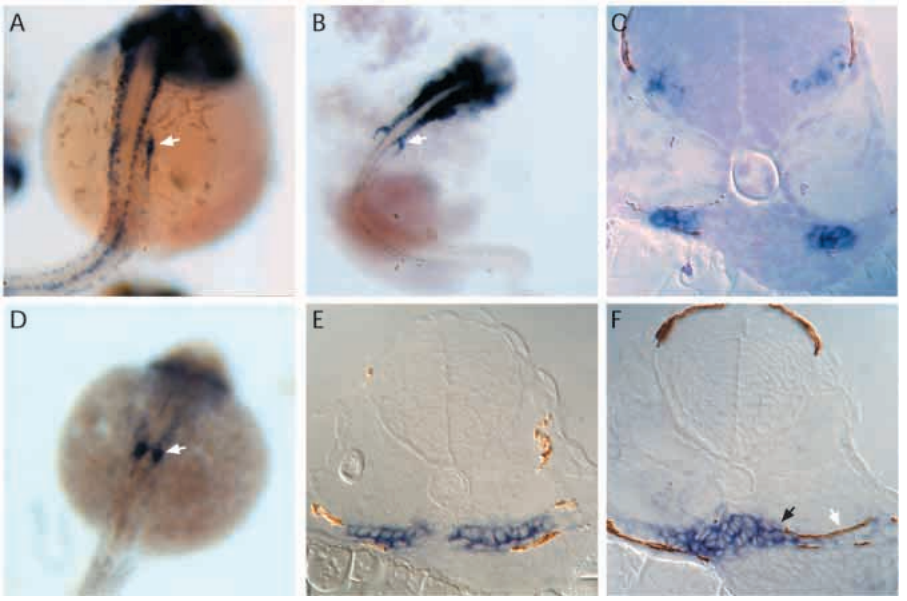

Fig. 3. Expression of *pax2.1* and *wt1* in the forming pronephros. (A) Whole-mount in situ hybridization shows *pax2.1* is expressed in the anterior pronephric ducts (arrow) at 24 h as well as in the spinal cord. (B) At 30-32 h, a new domain of *pax2.1* expression is observed anterior and medial to the pronephric ducts (arrow), in the position of the future pronephric tubules. (C) Histological sections of *pax2.1* expression in the presumptive tubule primordium cells show that these cells constitute the lateral half of the nephron primordium and that the medial halves of the nephron primordium are negative. (D) Whole-mount in situ hybridization shows *wt1* expression in the paired nephron primordia at 24h (arrow). (E) At 30-32 h, *wt1* is uniformly expressed throughout the nephron primordia. (F) By 36 h, *wt1* expression becomes restricted to a mass of cells at the midline in the position of the future glomerulus (black arrow). Lateral cells within the forming nephron in the position of the future tubule do not express *wt1* (white arrow).

partitioning of the nephron primordium at 30-40 hpf described in Fig. 2 correlates well with the expression of *pax2.1* specifically in the lateral pronephric tubule precursor cells and with the restriction of *wt1* expression to midline glomerular precursor cells (podocytes).

Ultrastructure of the pronephric glomerulus

The correlation between *wt1* expression in midline cells of the primordium and the encapsulation of these cells that occurs soon afterward suggests that, by 40 hpf, the forming glomerulus consists of encapsulated podocyte precursor cells. We examined embryos by electron microscopy to better assess this stage of podocyte cell differentiation and glomerular capillary development. Ultrastructure of the normal glomerulus at 40 hpf shows the formation of extensive podocyte foot processes and invagination of the basement membrane that encapsulates the podocytes (Fig. 4A). Also, cells lining the ventral aspect of the forming glomerulus have a characteristic flat appearance, suggestive of cells that go on to form the lining of Bowman's capsule (Fig. 4A). The results indicate that, by 40 hpf, the glomerular filtration apparatus is starting to form and that glomerular cells have begun to differentiate into podocytes (visceral epithelium) and the capsule lining (parietal epithelium). By 3.5 days postfertilization, development of the pronephric nephron is essentially complete (Fig. 4B). In electron micrographs of wild-type embryos at this stage, the glomerulus consists of densely packed capillaries surrounded by podocyte cell bodies with elaborate foot processes as well as mesangial cells containing prominent actin stress fibers (Fig. 4B). In most capillaries, the filtration barrier is well developed displaying an endothelium with open pores (without diaphragm), a thin trilaminar glomerular basement membrane, and podocytes with primary processes and numerous interdigitating foot processes.

Onset of glomerular filtration

Glomerular filtration is an essential element of renal function, generating the blood filtrate which is then selectively modified by transport processes in the renal tubules. The elaboration of foot processes and the infolding of the glomerular basement membrane at 40 hpf suggested that the onset of glomerular filtration may occur at or soon after this stage. To determine when glomerular filtration was first occurring, rhodamine dextran (10,000 M_r) was introduced into the circulatory system of wild-type embryos. If the glomerulus is functioning, this size of dextran should pass through the glomerular basement membrane and appear in the lumen of the pronephric duct. In 33-36 hpf embryos, no dye was found in the pronephric duct (data not shown). This suggests that (1) the opening to the coelom or transient nephrostome seen at earlier stages (Fig. 2A) is sealed by this time (i.e., no connection exists between the coelom and the pronephric duct) and (2) glomerular filtration has not yet begun. In 48 hpf embryos, injected dye is present in the lumen of the pronephric duct (Fig. 5A). In addition, ingrowth of the glomerular capillaries from the dorsal aorta is evident as fluorescent glomerular basement membranes (Fig. 5A,B). In 56 hour injected embryos, dye is present in the duct lumen as well as in brightly staining apical membrane vesicles in duct epithelial cells. Glomerular capillary development also becomes more elaborate (Fig. 5B). No dye is ever found in the lumen of other epithelial structures such as the gut, indicating that dye could not easily leak past epithelial cell junctions. These dye injection experiments suggest that glomerular filtration begins between 36 and 48 hours postfertilization and coincides with the elaboration of podocyte foot processes and the ingrowth of glomerular capillaries from the dorsal aorta.

Mutations affecting pronephric development

As part of a large-scale ENU mutagenesis screen for zebrafish developmental mutants (Driever et al., 1996), we have isolated eighteen independent recessive mutations affecting pronephric development. The visible unifying phenotype of all the mutants is the appearance of fluid-filled cysts in the region of the normal pronephros (Fig. 6A,B). These mutations comprise fifteen complementation groups (Table 1) and affect all three identifiable parts of the pronephros: the glomerulus, the tubule and the duct (see below). The relatively low alleles per locus

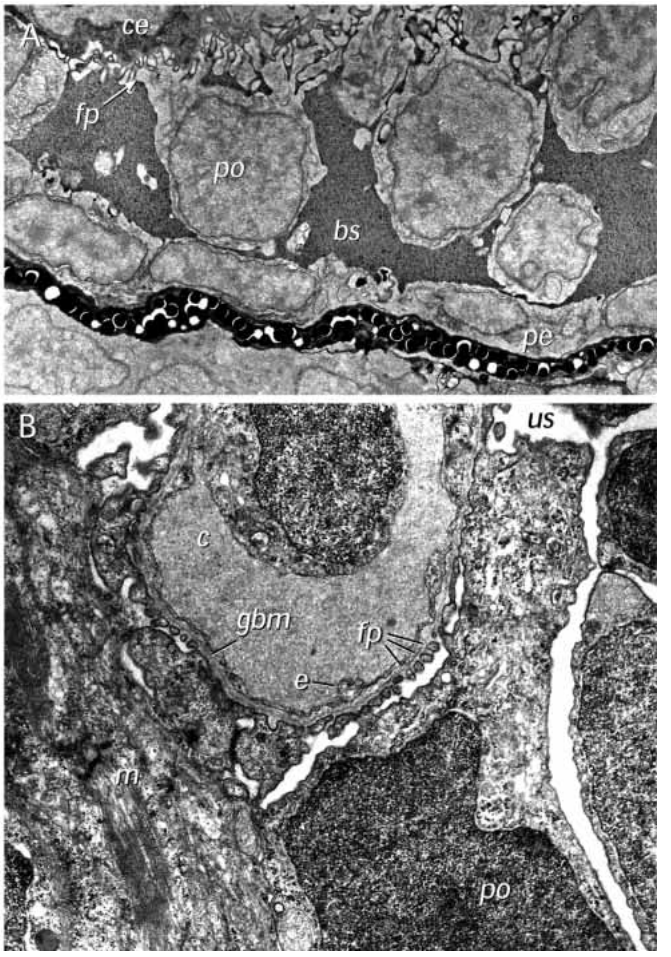

Fig. 4. Electron microscopy of the wild-type glomerulus. (A) Ultrastructure of the forming glomerulus at 40 hpf. A longitudinal section (similar to that presented in Fig. 2D) shows podocytes (*po*) extending foot processes (*fp*) in a dorsal direction and in close contact with capillary endothelial cells (*ce*). Bowman's space (*bs*) appears filled with an electron-dense precipitate and the ventralmost cells appear to be taking on the flattened appearance of the parietal epithelium (*pe*) that will line Bowman's capsule. (B) Glomerulus and filtration barrier of the wild-type pronephros at 3.5 days postfertilization. The filtration barrier is well developed displaying an endothelium with open pores (without diaphragm), a thin trilaminar glomerular basement membrane (*gbm*) and podocytes with primary processes and numerous interdigitating foot processes (*fp*). The filtration slits between the foot processes are bridged by one or sometimes two slit membranes. Mesangial cells (*m*) are also evident. *us*, urinary space; *c*, capillary space; *e*, endothelial cell. ×36,500.

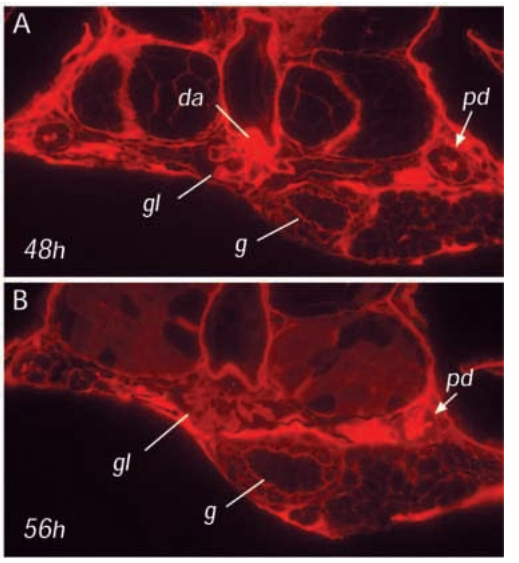

Fig. 5. Onset of glomerular filtration. (A) Wild-type embryos injected with rhodamine dextran (10,000 M_r) into the heart at 48 hpf show extensive accumulation of dye in interstitium and in basement membranes but not in the lumen of the gut (*g*). Dye is present in the lumen of the pronephric duct indicating that the pronephric filtration is functioning at this time. By 56 hpf (B), capillary invaginations in the glomerulus appear more extensive and dye can found in vesicles in the apical cytoplasm of the pronephric ducts. *da*, dorsal aorta; *gl*, glomerulus; *g*, gut; *pd*, pronephric duct.

rate (average alleles/locus = 1.2) within this group of mutants suggests that a much larger number of genes may be expected to contribute to this class of phenotypes.

Thirteen of the fifteen pronephric mutants recovered also manifest a pronounced ventral axis curvature (Fig. 6A) as well as bilateral pronephric cysts (Fig. 6B). Between 2 and 3 days of development, the cysts expand and bulge out behind the pectoral fins. With the exception of *pao pao tang* mutant embryos, which can survive for up to three weeks, all homozygous mutant embryos die by 5-6 days postfertilization with the larvae becoming grossly edematous. Since heart function appears to be normal in the mutant homozygotes, the edema is presumably due to a loss in pronephric function and failed osmoregulation. No developmental defects have been observed in heterozygotes. The degree of ventral axis curvature was found to be variable in individual clutches and when mutants were crossed to different genetic backgrounds. In some instances where axis curvature was not evident at all, the straight-bodied mutant homozygotes still developed cysts. In addition, at early stages of cyst formation (40 hpf; see below) ventral axis curvature in *dbb* homozygotes is limited to the growing tip of the tail and does not affect the trunk at all. The data suggest that cyst formation is not a consequence of axis curvature per se. It is more likely that the observed phenotypes are the consequence of a pleiotropic defect affecting both the pronephros and axis formation. The morphology of the pronephros in representative mutants in each class was examined.

double bubble was examined as a representative of the pronephric cyst/ventral axis curvature mutants. In 3.5-day-old *double bubble* (*dbb*^{m468}) homozygotes, large cysts are clearly evident in place of the glomerulus and pronephric tubule. The glomerulus appears as a flattened septum at the midline, studded with cell nuclei and with little enclosed vascular space (Fig. 6D). The cuboidal epithelium seen in the wild-type pronephric tubule (Fig. 6C) is either missing or severely flattened. *Fleer* (*flr*) manifests a similar cystic flattening of the pronephric tubule epithelium, although glomerular development is advanced to the stage of capillary loop formation (Fig. 6E). These loops, however appear grossly distended and aneurysmal. *Pao pao tang* exhibits a more localized defect in the pronephric tubule with the glomerulus

forming an apparently normal dense structure at the midline (Fig. 6F). Thus, despite an overt similarity in the formation of pronephric cysts, these mutations affect the different elements of the pronephros in discretely different ways.

The largest group of mutants (Table 1) all show a phenotype similar to *double bubble*. These mutants manifest cysts soon after hatching, develop severe edema and display an axis curvature defect. As a representative of this group, *double bubble* was chosen for a more detailed analysis. The defects in the glomerulus and the absence of a normal pronephric tubule epithelium at 3.5 dpf suggested that the *dbb* mutation may affect both glomerular and tubule cell differentiation, with cyst formation occurring in both structures simultaneously. Alternatively, cyst formation could be initiated first in either the glomerulus or the tubules, with secondary involvement in the neighboring structures. To distinguish between these possibilities, we examined mutant pronephroi prior to the appearance of cysts. Homozygous mutant embryos were identified prior to cyst formation by virtue of the co-segregating curly tail phenotype at 30 hpf.

Glomerular defects in *dbb*

By histology, the nephron primordium cells of *dbb*^{m468} homozygotes are normal at 33 hpf (Fig. 7A). Consistent with this normal morphology, the expression of *wt1*, a marker of podocyte differentiation, is indistinguishable from wild-type siblings (data not shown). However, by 40 hpf aberrations in glomerular structure are evident. The capsule that divides the presumptive glomerulus from the forming tubule cells is not present. Instead, areas of cellular thinning are present at the junction of the glomerulus and pronephric tubule (Fig. 7B). The increased space between cells suggested that the glomerulus is starting to fill with fluid and expand. Pronephric tubule cells do not appear to be excessively flattened or morphologically abnormal at this stage (Fig. 7B). Longitudinal views of the same structure show the extent of glomerular swelling as well as a flattening of glomerular cells and an increased incidence of podocyte cytoplasmic extensions into the lumen (Fig. 7C). By 56 hpf, the glomerulus appears loose and distorted with cystic space expanding laterally (Fig. 7D). The morphology of the *dbb*$^{m468-/-}$ pronephros suggests that cyst formation is most closely associated with early defects in glomerular structure.

By EM, at 40 hpf the extent of foot process formation and basement membrane invagination appears reduced or possibly delayed (Fig. 8A), and the lumen or presumptive urinary space of the mutant glomerulus is expanded. The formation of glomerular cysts in 40 hour *dbb*$^{-/-}$ embryos coincides temporally with the onset of glomerular filtration and suggests that filtration pressure may play a role in the deformation of the pronephros.

By 3.5 days, the glomerulus of *dbb*^{m468} homozygotes appears as a flattened, podocyte lined septum at the midline juxtaposed between the expanded pronephric cysts (Fig. 8B). Despite its disorganized appearance, the mutant glomerulus still retains a variety of recognizable glomerular cell types. Podocytes and foot processes can be seen surrounding distended capillaries (Fig. 8B). Endothelial cells lining the capillaries and mesangial cells in interstitial space are present (Fig. 8B). The podocyte layer continues into the outer sheet of Bowman's capsule. Some distance beyond the bend, the epithelium transitions into the thin parietal epithelium. This epithelium consists of simple polygonal cells and is equivalent to the wall of the cysts; at this stage of cyst development, there is no indication of a normal

Table 1. Zebrafish pronephric kidney mutants

Mutant	Alleles
Pronephric cyst, body axis curvature	
double bubble (*dbb*)	m468, m153, & m587
bazooka Joe (*bzj*)	m453, & m527
dizzy (*dzz*)	m605
junior (*jnr*)	m304
mr. bubble (*mrb*)	m305
blowup (*blp*)	m348
fusen (*fsn*)	m478
bubblicious (*bcs*)	m620
big league chew (*ble)*	m696
hubba bubba (*hba*)	m194
inflated (*ifl*)	m786
Pronephric tubule cyst	
pao pao tang (*pap*)	m629
cyster (*cst*)	m329
Pronephric cyst, body axis curvature, eye degeneration	
fleer (*flr*)	m477
elipsa (*eli*)	m649

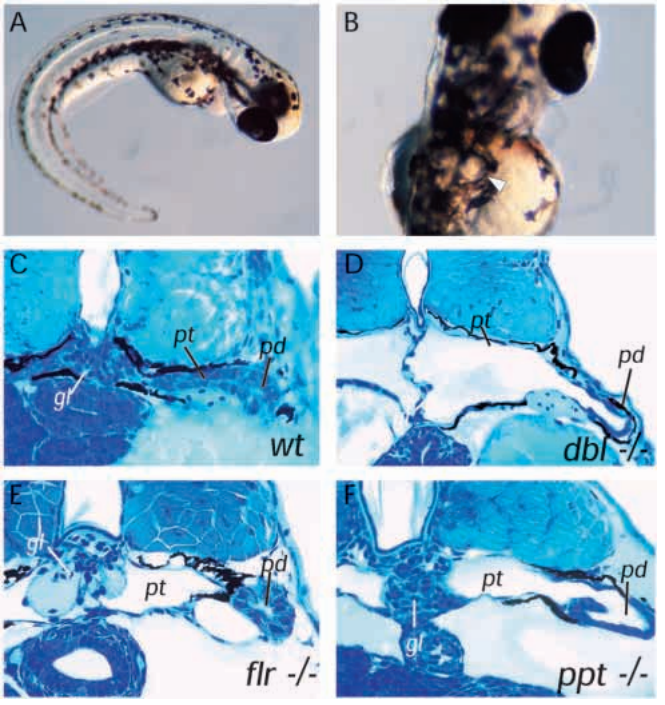

Fig. 6. Cystic maldevelopment in zebrafish pronephric mutants. (A) The mutant *double bubble* (*dbb*$^{m153)}$ emerges from its chorion with a ventrally curved body axis and within 3-4 hours bilateral pronephric cysts (arrow in B) are evident. (C) Cross section of wild-type pronephros at 3.5 days pf. (D) Section of *dbb*^{m468} showing a grossly distended pronephric cyst in place of the pronephric tubule and a glomerulus reduced to a flattened septum at the midline. (E) The mutant *fleer* (*flr*) shows less severe cyst distension despite a flattened pronephric tubule epithelium and also a marked distension of the glomerular capillaries. (F) *pao pao tang* (*pap*) has an apparently intact glomerulus while the pronephric tubule epithelium is flattened and the pronephric duct is also distended. *gl*, glomerulus; *pt*, pronephric tubule; *pd*, pronephric duct.

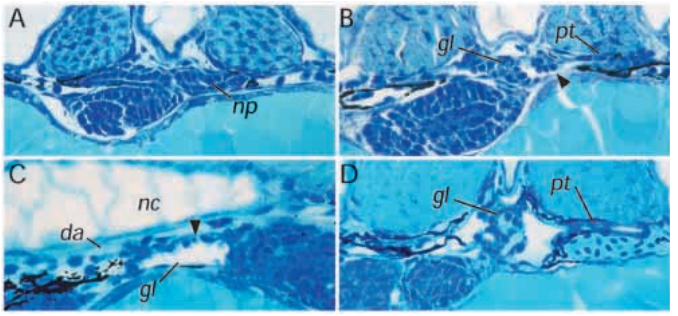

Fig. 7. Early glomerular defects in the *dbb*$^{-/-}$ pronephros. *dbb*$^{m468-/-}$ embryos were examined at different stages of nephron development to determine the site of the primary defect. (A) Cross sections of *dbb*^{m468} pronephroi at 33 hpf reveal that the nephron primordium (*np*) is a double-layered sac of cells with a central lumen similar to wild-type pronephroi at this stage. (B) In 40 hpf mutant pronephroi, the distinct basement membrane separating glomerular and tubule domains is not seen. Instead, the forming glomerulus appears distended with fluid and cell-free areas (arrow) are evident at the junction of the glomerulus and tubule. (C) Longitudinal sections through the mutant glomerulus shows a distension of the glomerular lumen, flattening of glomerular cells and a thinning of cells associated with the glomerular basement membrane (arrow). (D) At 2.5 dpf, the *dbb*^{m468} pronephros displays a loose and disorganized glomerulus with progressive distension of the pronephric tubule. *gl*, glomerulus; *pt*, pronephric tubule; *pd*, pronephric duct; *nc*, notochord; *da*, dorsal aorta.

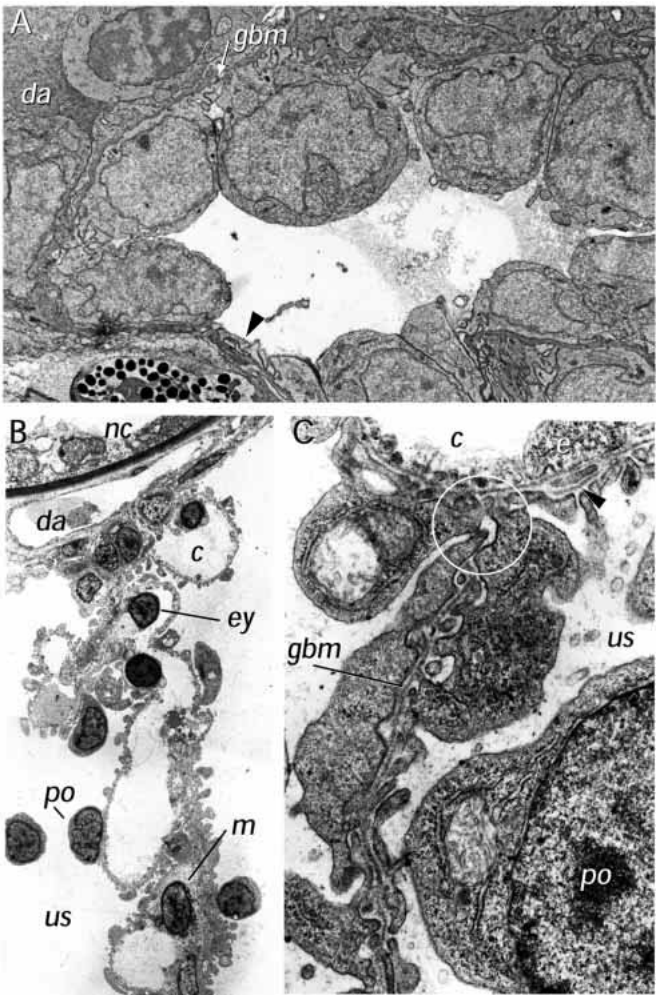

Fig. 8. Ultrastructure of the *dbb*$^{-/-}$ glomerulus. (A) Ultrastructure of the *dbb*$^{-/-}$ glomerulus at 40 hpf. Podocytes (*po*) are present but appear to show less extensive podocyte foot process development at this stage compared to wild type. Areas of cellular thinning (arrow) are also evident. (B) Cross section of the glomerular septum in the mutant double bubble (3.5 dpf). The glomerular capillaries (*c*), mesangium (*m*) and podocytes (*po*), on either side form a medial septum between the two cysts. The urinary spaces (*us*) on both sides of the septum represent the lumens of the cysts. ×3,500 (C) Section of part of the *dbb*$^{m468-/-}$ glomerular septum extending between two capillaries (*c*), (only one capillary is shown at the top). In several places, the glomerular septum consists of two podocyte layers (*po*) located adjacent to each other without a capillary or a mesangial layer in between. The two epithelia are focally interconnected by cell-cell junctions and form a common glomerular basement membrane (*gbm*), which appears not to be continuous with the GBM of the adjacent glomerular capillaries (encircled). In some places, the GBM appears to split and rejoin (arrowhead). ×35 000. *da*, dorsal aorta; *gbm*, glomerular basement membrane; *nc*, notochord; *e*, capillary endothelial cell; *ey*, erythrocyte; *c*, capillary lumen; *us*, urinary space.

cuboidal pronephric tubule epithelium (data not shown). Although typical glomerular cell types are present, their organization and the overall architecture of the glomerulus was severely distorted. In some areas, podocytes can be seen in close apposition to each other on either side of a single basement membrane (Fig. 8C), a configuration never seen in normal embryos. In several areas, the mutant GBM appears thin and discontinuous. Splitting of the GBM is also seen in mutant embryos (Fig. 8C) but never in wild type.

The abnormalities in the forming glomerulus and also in the glomerular basement membrane at later stages suggest that the mutation in *dbb* may play a direct role in glomerulogenesis. Alternatively, the expansion of the glomerulus could be a secondary consequence of a more distal defect in the pronephros such as obstruction of the pronephric duct. We therefore examined the cloaca in whole fish for any signs of lumen blockage. We also examined the duct in ten individual *dbb* homozygotes by serial sectioning the entire rostral-caudal extent of the pronephros. The results indicate that the lumen in all *dbb* homozygotes examined remains patent all the way to the cloaca (Fig. 9A,B). The examination of whole fish is confirmed by histological sections (Fig. 9C) which show a patent lumen all the way back to the point where the bilateral pronephric ducts fuse. Additional sections in different planes did not show any blockage. We conclude from this that the *dbb* mutation causes an intrinsic defect in the forming pronephros and that cyst expansion is not secondary to blockage of the pronephric duct.

Membrane protein targeting defects in pronephric mutants

In *dbb* and similar pronephric mutants, the pronephric duct appeared distended although not overtly cystic. Epithelial cell differentiation in the pronephric duct was determined by assessing the degree of cell membrane polarization. The Na^+/K^+ ATPase is a membrane-bound ion pump normally located basolaterally in kidney tubule and collecting system

epithelia, consistent with its role in electrolyte and solute resorption from the glomerular filtrate. Alkaline phosphatase (AP) is an ectoenzyme normally located on the apical surfaces of pronephric duct cells. In whole-mount 2.5 dpf embryos stained with the anti-Na^+/K^+ ATPase alpha subunit monoclonal alpha6F, both wild-type and *dbb*^{m468} homozygotes showed strong immunoreactivity in the pronephric duct (Fig. 10A,B). Sections of wild-type embryos show that Na^+/K^+ ATPase immunoreactivity is restricted to the basolateral surfaces of pronephric duct epithelial cells (Fig. 10C). In contrast, several of the pronephric mutants show altered localization of the Na^+/K^+ ATPase. In *dbb*^{m468}, staining is primarily apical while basolateral cell surfaces show greatly reduced staining (Fig. 10D). *flr* also shows this reversed pattern of staining (Fig. 10E) while other mutants show an intermediate phenotype of lateral staining with apical and basal cell surfaces being negative (Fig. 10F-H).

To assess whether mutant duct cells had completely lost their polarity, we stained for endogenous alkaline phosphatase activity. In wild-type embryos there is a tight lumenal ring of AP staining on the apical duct cell surfaces (Fig. 10I). In *dbb*^{m468}, *ifl* or *dzz* homozygotes, AP staining is normal in its restriction to the apical surface (Fig. 10J). These results indicate the mutant duct cells retain control mechanisms that generate apical cell polarity but fail to target or retain the alpha 6F antigen on the basolateral cell surface.

Additional phenotypes associated with pronephric cyst mutants

With the exception of *pao pao tang* (*pap*; m629) and *cyster* (*cst*; m329), all mutants in this group consistently manifested a curved body axis (Fig. 6A). The direction of curvature was highly variable; some embryos had a predominate downward curvature while mutant siblings would show lateral curvature or a sinusoid axis (data not shown). Development of this defect is not dependent on the constraints of developing within a rigid chorion since de-chorionated mutant embryos also develop curvature. No obvious defects in notochord development were observed in any of the mutants and in the two mutants examined (*dbb*^{m468} and *dzz*), the presence of a floor plate and hypochord was indicated by expression of collagen type II (data not shown). The structural defect underlying the axis curvature is currently not known. Two mutants, *flr* and *elipsa*, showed late developmental defects in the eye. The eye develops normally to 3 days; all cell layers appeared normal. However, between 3.5 and 5 days of development apoptotic cells appear in the photoreceptor cell layer (Fig. 11A,B). This phenotype is essentially identical to the previously described phenotype of *elipsa* (Malicki et al., 1996). In complementation tests, *flr* and *elipsa* are not allelic. These results suggest that *flr* and *elipsa*

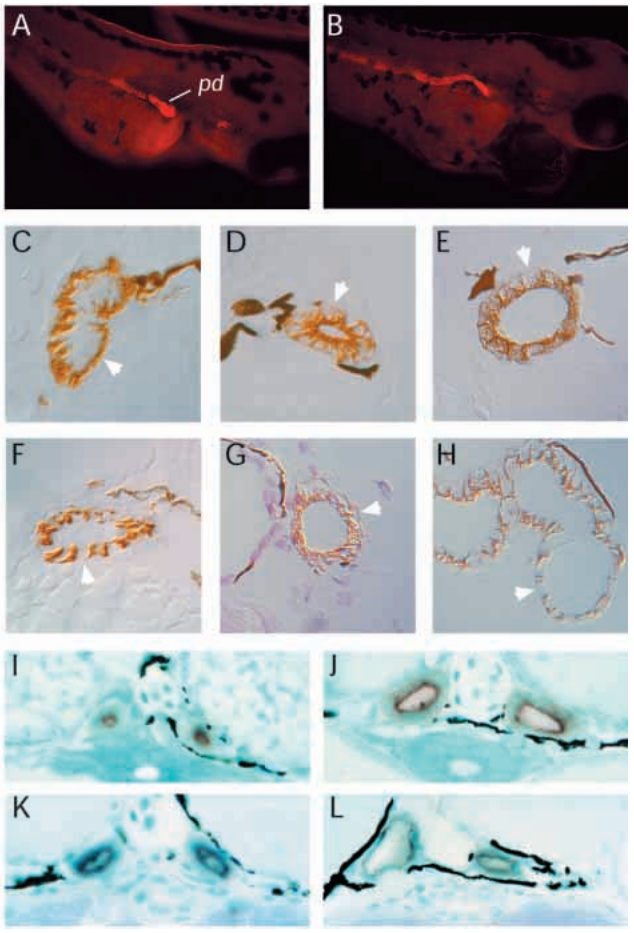

Fig. 10. Altered membrane protein targeting in pronephric mutants. (A) The monoclonal antibody alpha6F raised against the chicken alpha-1 subunit of the Na^+/K^+ ATPase reacts strongly with the pronephric duct (*pd*) at hatching (2.5 days) in wild-type (A) and mutant (*dbb*^{m468}) (B) whole-mount embryos. In sections of wild-type duct (C), alpha6F staining is exclusively basolateral (arrow) while, in *dbb* (D), alpha6F staining is strongly apical and diminished on basolateral membranes (arrow). Diminished alpha6F basolateral staining is also observed in (E) fleer (*flr*), (F) dizzy (*dzz*), (G) inflated (*ifl*) and (H) big league chew (*chw*) mutant duct cells. (A,B) Cy3-labeled secondary antibody; (C-H) HRP-labeled secondary antibody. (I-L) Endogenous alkaline phosphatase staining is apical in wild-type pronephric duct (I) and is not affected in *dbb* (J), inflated (*ifl*) (K), or dizzy (*dzz*) (L), mutant duct cells.

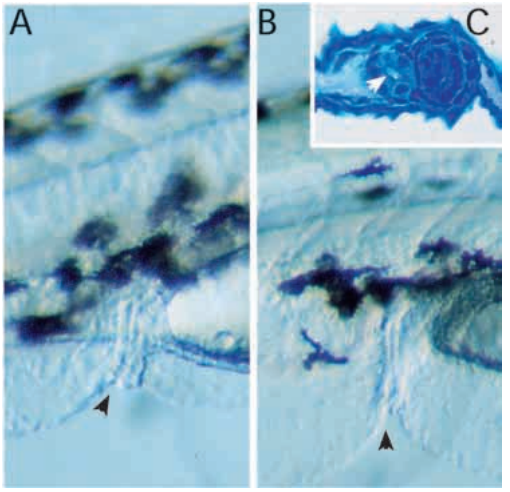

Fig. 9. The pronephric duct is not obstructed in *dbb*$^{-/-}$ embryos. The lumen of the pronephric duct and cloaca is visible and patent in both wild-type (A) and *dbb* mutant (B) embryos indicating a lack of obstruction to the flow of fluid from the pronephros. (C) Serial sections show a patent pronephric duct lumen (arrow) in *dbb* homozygotes.

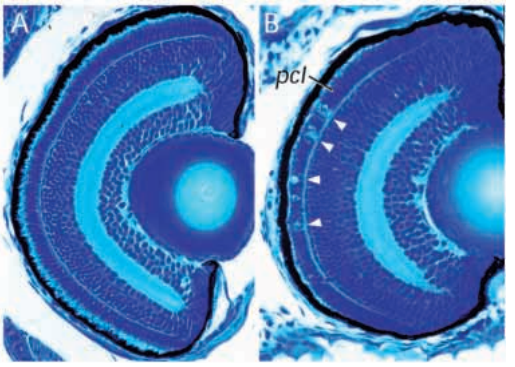

Fig. 11. Eye defects in *fleer*$^{-/-}$ embryos. (A) Section of a wild-type eye at 72 hpf showing the characteristic stratification of retinal cell layers. (B) *fleer* mutant embryos at 72 hpf show excessive cell death in the photoreceptor cell layer (*pcl*; arrows).

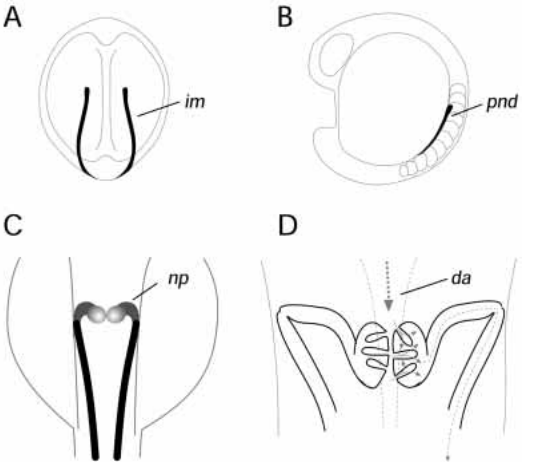

Fig. 12. Developmental stages in the formation of the zebrafish pronephros. (A) 1- to 8-somite stage (10-13 hpf). Expression patterns of *pax2.1* and *lim-1* define the posterior regions of the intermediate mesoderm (*im*) and suggest that a nephrogenic field is established early in development. (B) Early somitogenesis to Prim-5 stage (12-24 hpf). Growth of the pronephric duct (*pnd*) follows behind somitogenesis and is complete by 24 hpf. Nephron primordia form at the anterior tips of the pronephric ducts by 24 hpf. (C) Prim-5 to High-Pec stage (24-42 hpf). Nephron primordia (*np*) ventral to somite three separate from the coelom and undergo integrated morphogenesis, giving rise to pronephric glomeruli and tubules. (D) High-Pec stage to Hatching (42-48 hpf). Vascularization of the pronephros by ingrowth of capillaries from the dorsal aorta (*da*) starts at 40-42 hpf and continues over the next 24 h and correlates with the onset of glomerular filtration. Stages of zebrafish development refer to Kimmel et al. (1995).

are two different genes involved in similar pathways required for development of the pronephros, proper body axis and survival of cells in the eye.

DISCUSSION

Our goal in undertaking this work was to explore the molecular mechanisms that underlie the formation and function of the zebrafish pronephros, as an example of a simple vertebrate kidney. We have established the stages of zebrafish pronephric development and the onset of pronephric function, and have characterized mutations affecting the architecture and function of the glomerulus and the genesis of cell membrane polarity.

Pronephric development

Our results, together with previous studies, show that the zebrafish pronephros is formed in discrete stages which may be described as (1) early specification of the nephrogenic cell lineage (Fig. 12A), (2) growth and differentiation of the pronephric ducts (Fig. 12B), (3) formation and differentiation of the nephron primordia (Fig. 12C) and (4) vascularization of the glomerulus and the onset of blood filtration (Fig. 12D).

Specification of the nephrogenic cell lineage

Previous fate mapping studies in zebrafish have identified gastrula stage cells in the deep cell layer, just ventral to the heart progenitors, which are fated to become the pronephros (Kimmel et al., 1990). Later, at about the 1-somite stage, bilateral bands of intermediate mesoderm can be identified by the expression of the transcription factors *pax2.1* and *lim1* (Fig. 12A; Krauss et al., 1991; Toyama and Dawid, 1997). The continuity of expression of these genes later in the forming pronephros suggests that the early *pax2.1/lim1* expression domain may define the zebrafish nephrogenic field.

Growth of the pronephric duct

Originating from tissue lying ventral to the third somite, the pronephric duct grows caudally under the newly formed somites (Fig. 12B; Kimmel et al., 1995). By 24 hours of development, the duct forms a patent epithelial tube exiting the embryo behind the yolk extension (Kimmel et al., 1995). In *fundulus heteroclitus*, the pronephric duct at a similar stage, prior to glomerular development, has been shown to be already functional in the secretion of organic anions (Armstrong, 1932). This form of transepithelial secretion (Dantzler, 1989) may also be active in the zebrafish pronephric duct given that crystalline deposits (possibly urate salts; Nussbaum, 1886) are often observed in the lumen of the newly formed duct (Kimmel et al., 1995).

Formation and differentiation of the nephron primordia

At 24 hpf, the tissue that will later form the pronephric tubules and the glomerulus exists as paired, disk-shaped primordia ventral to the third somite directly abutting on the anterior tip of the pronephric duct. The relatively undifferentiated morphology of the primordia and the fact that cells of the primordia express *lim1* (Toyama and Dawid, 1997) as well as *wt1* suggest a relationship to the cells of the condensed mesenchyme or primary renal vesicle observed in metanephric development which also express *wt1* and *lim-1* (Buckler et al., 1991; Armstrong et al., 1993; Fujii et al., 1994; Karavanov et al., 1998). However, in the zebrafish pronephros, as well as in the in the *Xenopus* nephric system, *wt1*-expressing cells have a distinctly different origin, being derived from mesoderm adjacent to the coelom as opposed to the loose metanephric mesenchyme (Goodrich, 1930; Marshall and Smith, 1930; Armstrong, 1932; Saxén, 1987; Carroll and Vize, 1996; Semba et al., 1996). Nonetheless, the expression of *lim1* and *wt1* in

the primordia at this stage suggests that similar developmental events may be occurring in these different kidney forms.

Between 30 and 40 hours of development, the nephron primordium is separated from the coelom and morphogenesis of the nephron occurs (Fig. 12C) with the formation of distinct tubular domains laterally and glomerular domains in apposition to the dorsal aorta at the embryo midline. Expression of *pax2.1* at 30-32 hpf in the lateral cells of the nephron primordium is the earliest sign of tubule cell differentiation while restriction of *wt1* expression to cells at the midline (36 hpf) correlates with podocyte differentiation soon after (40 hpf). This stage, where the nephron primordium is patterned but is not yet vascularized, is conceptually equivalent to the S-shaped body stage in the development of the metanephric nephron (Saxén, 1987). Similar patterns of *pax2* and *wt1* gene expression in the corresponding tissues of the amphibian pronephros have also been observed although the timing and spatial relationship of expression differs from the zebrafish pronephros. In *Xenopus*, *pax2* expression in the pronephric tubules occurs simultaneously with the caudal growth of the duct while, in zebrafish, expression of *pax2.1* in the forming tubules occurs after duct formation is complete. Secondly, the zebrafish pronephros is an integrated nephron system (lacking nephrostomes) where the tubule and glomerulus differentiate in intimate contact. In *Xenopus*, primordia of the glomus and tubule are more distinctly separate. It is not known whether these differences are developmentally significant; similar developmental mechanisms may well be operating in the formation of the teleost and amphibian pronephroi. These mechanisms, at least at the cellular level, are likely to involve some of the same molecular signals that pattern the metanephric kidney (Vize et al., 1997). The relative simplicity of the pronephros and these differences in timing of nephron formation provide an opportunity to further clarify developmental mechanisms specific to tubule and glomerular cell differentiation.

Vascularization of the glomerulus

Between 40 and 48 hours of development, the interaction between the emerging podocyte foot processes and capillaries growing in from the dorsal aorta establishes the glomerular blood filter (Fig. 12D). These morphological changes occur just prior to hatching and coincide with the onset of glomerular function. Also, by this stage, a distinct proximal brush border segment in the pronephric tubule is formed (Hentschel and Elger, 1996). Pronephric glomerular development in zebrafish is similar to that described for other teleosts although the timing of glomerular development, relative to hatching, has been found to vary widely (Marshall and Smith, 1930; Armstrong, 1932; Newstead and Ford, 1960; Agarwal and John, 1988; Tytler et al., 1996). The larval zebrafish pronephros is thus composed of two nephrons which, despite their simplicity, possess relevant kidney cell types, express well-conserved regulators of nephrogenesis and form tissue structures that are common to all vertebrate kidneys.

Cystic maldevelopment in zebrafish pronephric mutants

The mutations that we analyzed identify 15 different genes that are essential for the proper structure and functioning of the pronephros. The development of pronephric cysts in these mutants followed by general edema raises obvious questions concerning the primary defects responsible for cyst formation. Obstruction or extirpation of the pronephric duct in amphibians will cause tubule dilation followed by general edema (Howland, 1921; Fales, 1935) due to loss of osmoregulation. We found no evidence for obstruction of filtrate flow in *dbb* homozygotes by serial histological section of the pronephric duct or by examination of whole fish. Distal obstruction of the higher vertebrate kidney primarily affects the collecting system (hydronephrosis; (Klahr and Harris, 1992)) while our observations suggest that the glomerulus is the first part of the zebrafish pronephros affected in the mutants, followed secondary involvement of the tubules and ducts. In addition, in *noi* homozygotes, which we find specifically lack pronephric tubules and therefore lack any egress for blood filtrate, glomerular development is relatively normal and does not become cystic (unpublished results). For these reasons, it is unlikely that obstruction is the primary cause of pronephric cyst formation in the pronephric mutants. Is cyst formation a response to general edema? Cyst formation begins early during glomerular development (40 hpf) at a time there is no general edema. In fact, general edema is not observed until day 3 of development. Even in mutants such as *silent heart*, which develops a pronounced cardiac edema by day 3, we find that the pronephros does not become dilated as it does in *dbb* for instance (unpublished results). It is more likely that the general edema observed in the pronephric cyst mutants is a consequence of pronephric failure and altered osmoregulation. Is cyst formation secondary to axial defects in the curly tail mutants? As noted in the results, we find that axis curvature in *dbb* is seen only in the tip of the tail at 40 hpf and does not affect the trunk at the time of cyst formation. Also on some genetic backgrounds, the axis curvature phenotype is greatly diminished while cyst formation is not affected. Although it is possible that axial structures may play a role in pronephric development, we find that, in the mutant *floating head*, which completely lacks a notochord and notochord-induced axial structures, a pronephros still forms and does not become cystic (unpublished results). It is therefore likely that the pronephric and axis defects in *dbb* and other pronephric mutants are the result of a mutation in a pleiotropically active gene.

Pronephric mutants as models of glomerular development and function

Our analysis of the *double bubble* mutation, as a representative of the largest group of pronephric mutants, suggests that a primary defect may be in the formation of the glomerulus. The distension of the glomerulus at a time when blood filtration is just getting established as well as the defects in the glomerular basement membrane observed later in development raises the possibility that cyst development in *dbb* may be related to an inability to withstand filtration pressure followed by progressive distension of the pronephric tubule and duct epithelia. The glomerular basement membrane in vertebrate kidneys is composed primarily of heparan sulfate proteoglycan, laminin and a cross-linked network of type IV collagens. In addition to providing a structural scaffold for cellular interaction in the glomerulus, the character of the GBM defines the function of the glomerular filter through which blood plasma passes into the urinary space (Saxén, 1987). Alteration in specific matrix molecules, such as type IV

collagen subunits and laminin β2, results in loss of filtration properties as evidenced by the occurrence of proteinuria in Alport's syndrome (Zhou et al., 1991; Miner and Sanes, 1996). However, mouse and human mutations in either of these genes do not lead to kidney cyst formation (Noakes et al., 1995; Miner and Sanes, 1996). Glomerulocystic kidneys have been observed associated with mutations in the PKD1 gene, which accounts for the majority of cases of autosomal dominant polycystic kidney disease (ADPKD) in humans (Torra et al., 1997). ADPKD has also been associated with apical mislocalization of the Na^+/K^+ ATPase (Wilson et al., 1991) not unlike what we observe in larvae homozygous for the *double bubble* and *fleer* mutations. At present, however, there is no evidence that any of these zebrafish mutants harbor defects in homologs of human PKD genes.

Pronephric mutants as models of terminal epithelial cell differentiation

The generation of epithelial cell polarity is thought to be the result of a hierarchical process guided both by environmental signals and by spatial cues intrinsic to the cell (Drubin and Nelson, 1996). The multiple steps involved in the initiation and maintenance of cellular polarity include cell adhesion to matrix, the formation of cell-cell junctional complexes, the alignment of cytoplasmic organelles and the cytoskeleton and, finally, maintenance of membrane asymmetry by proper intracellular vesicle targeting (Drubin and Nelson, 1996). It is possible that failure at any one of these stages could result in the loss of some or all aspects of epithelial cell polarity. The mislocalization of the Na^+/K^+ ATPase alpha subunit to the apical cytoplasm of the pronephric duct in *double bubble*, *fleer* and other mutants suggests that, in addition to their function in glomerular development, the *dbb* and *flr* genes may also be required in tubule and duct epithelia for proper terminal cell differentiation and the generation of epithelial cell polarity. Our results suggest that markers of apical polarity are unaffected in *dbb* but that basolateral polarity is specifically lost. The *dbb* gene may be required for correct targeting or maintenance of a specific subset of membrane proteins in basolateral cell membranes. Further analysis of *dbb*, *flr* and other genes described here using additional markers of cell polarity and an assessment of whether they act cell-autonomously is likely to elucidate essential mechanisms underlying cell polarity and terminal epithelial cell differentiation.

We thank Colleen Boggs for maintaining the zebrafish facility at MGH. We also thank Dennis A. Ausiello for constant support, Aiping Liu for her contribution to the early stages of this work, Peg McGlaughlin and Mary McKee for expert assistance with electron microscopy and Brandon Sullivan for suggestions for mutant names. This work was supported in part by NIH R01 DK53093-01 (I. A. D.), the Deutsche Forschungsgemeinschaft (E1 92/3-2) and the Max-Planck-Gesellschaft (H. H. and M. E.) and a sponsored research agreement with Bristol Myers-Squibb (to M. C. F. and W. D.).

REFERENCES

Agarwal, S. and John, P. A. (1988). Studies on the development of the kidney of the guppy, *Lebistes reticulatus*. Part 1. The development of the pronephros. *J. Anim. Morphol. Physiol.* **35,** 17-24.

Agarwal, S. and John, P. A. (1988). Studies on the development of the kidney of the guppy, *Lebistes reticulatus*. Part 2. The development of the mesonephros. *J. Anim. Morphol. Physiol.* **35,** 24-30.

Armstrong, J. F., Pritchard-Jones, K., Bickmore, W. A., Hastie, N. D. and Bard, J. B. (1993). The expression of the Wilms' tumour gene, WT1, in the developing mammalian embryo. *Mech. Dev.* **40,** 85-97.

Armstrong, P. B. (1932). The embryonic origin of function in the pronephros through differentiation and parenchyma-vascular association. *Am. J. Anat.* **51,** 157-188.

Brand, M., Hesenberg, C.-P.,Warga, R., Pelegri, F., Karlstrom, R. O., Beuchle, D., Picker, A., Jiang, Y.-J., Furutani-Seiki, M., van Eeden, F. J. M. and others (1996). Mutations affecting development of the midline and general body shape during zebrafish embryogenesis. *Development* **123,** 129-142.

Buckler, A. J., Pelletier, J., Haber, D. A., Glaser, T. and Housman, D. E. (1991). Isolation, characterization, and expression of the murine Wilms' tumor gene (WT1) during kidney development. *Mol. Cell Biol.* **11,** 1707-1712.

Carroll, T. J. and Vize, P. D. (1996). Wilms' tumor suppressor gene is involved in the development of disparate kidney forms: evidence from expression in the Xenopus pronephros. *Dev. Dyn.* **206,** 131-138.

Chen, J. N., Haffter, P., Odenthal, J., Vogelsang, E., Brand, M., van Eeden. F. J. M., Furutani-Seiki, M., Granato, M., Hammerschmidt, M. and others (1996). Mutations affecting the cardiovascular system and other internal organs in zebrafish. *Development* **123,** 293-302.

Dantzler, W. H. (1989). Organic acid (or anion) and organic base (or cation) transport by renal tubules of nonmammalian vertebrates. *J. Exp. Zool.* **249,** 247-257.

Dent, J. A., Polson, A. G. and Klymkowsky, M. W. (1989). A whole-mount immunocytochemical analysis of the expression of the intermediate filament protein vimentin in Xenopus. *Development* **105,** 61-74.

Dressler, G. R. and Douglass, E. C. (1992). Pax-2 is a DNA-binding protein expressed in embryonic kidney and Wilms tumor. *Proc. Natl Acad. Sci. USA* **89,** 1179-1183.

Driever, W., Solnica-Krezel, L., Schier, A. F., Neuhauss, S. C. F., Malicki, J., Stemple, D. L., Stainier, D. Y. R., Zwartkruis, F., Abdelilah, S., Rangini, Z. and others (1996). A genetic screen for mutations affecting embryogenesis in zebrafish. *Development* **123,** 37-46.

Drubin, D. G. and Nelson, W. J. (1996). Origins of cell polarity. *Cell* **84,** 335-344.

Dudley, A. T., Lyons, K. M. and Robertson, E. J. (1995). A requirement for bone morphogenetic protein-7 during development of the mammalian kidney and eye. *Genes Dev.* **9,** 2795-2807.

Fales, D. E. (1935). Experiments on the development of the pronephros of *Ambystoma punctatum*. *J. Exp. Zool.* **72,** 147-173.

Fujii, T., Pichel, J. G., Taira, M., Toyama, R., Dawid, I. B. and Westphal, H. (1994). Expression patterns of the murine LIM class homeobox gene lim1 in the developing brain and excretory system. *Dev. Dyn.* **199,** 73-83.

Goodrich, E. S. (1930). Studies on the structure and development of vertebrates. London: Macmillan.

Haffter, P., Granato, M., Brand, M., Mullins, M. C., Hammerschmidt, M., Kane, D. A., Odenthal, J., van Eeden, F. J. M., Jiang, Y.-J., Heisenberg, C.-P. and others (1996). The identification of genes with unique and essential functions in the development of the zebrafish, Danio rerio. *Development* **123,** 1-36.

Hatini, V., Huh, S. O., Herzlinger, D., Soares, V. C. and Lai, E. (1996). Essential role of stromal mesenchyme in kidney morphogenesis revealed by targeted disruption of Winged Helix transcription factor BF-2. *Genes Dev.* **10,** 1467-1178.

Heller, N. and Brandli, A. W. (1997). Xenopus Pax-2 displays multiple splice forms during embryogenesis and pronephric kidney development. *Mech. Dev.* **69,** 83-104.

Hentschel, H. (1991). Developing nephrons in adolescent dogfish, Scyliorhinus caniculus (L.), with reference to ultrastructure of early stages, histogenesis of the renal countercurrent system, and nephron segmentation in marine elasmobranchs. *Am. J. Anat.* **190,** 309-333.

Hentschel, H. and Elger, M. (1996). Functional morphology of the developing pronephric kidney of zebrafish. *J. Amer. Soc. Nephrol.* **7,** p. 1598.

Howland, R. B. (1921). Experiments on the effect of the removal of the pronephros of *Ambystoma punctatum*. *J. Exp. Zool.* **32,** 355-384.

Humphrey, C. and Pittman, F. (1974). A simple methylene blue-azure II-basic fuchsin stain for epoxy-embedded tissue sections. *Stain Technol.* **49,** 9-14.

Jaffe, O. C. (1954). Morphogenesis of the pronephros of the leopard frog (*Rana Pipiens*). *J. Morphology* **94,** 109-123.

Karavanov, A. A., Karavanova, I., Perantoni, A. and Dawid, I. B. (1998). Expression pattern of the rat Lim-1 homeobox gene suggests a dual role during kidney development. *Int. J. Dev. Biol.* **42,** 61-66.

Kimmel, C. B., Ballard, W. W., Kimmel, S. R., Ullmann, B. and Schilling, T. F. (1995). Stages of embryonic development of the zebrafish. *Dev. Dyn.* **203,** 253-310.

Kimmel, C. B., Warga, R. M. and Schilling, T. F. (1990). Origin and organization of the zebrafish fate map. *Development* **108,** 581-594.

Klahr, S. and Harris, K. P. G. (1992). Obstructive Uropathy. In *The Kidney. Physiology and Pathophysiology.* (ed. Seldin and Giebisch), 3327-3369. New York: Raven Press.

Krauss, S., Johansen, T., Korzh, V. and Fjose, A. (1991). Expression of the zebrafish paired box gene pax[zf-b] during early neurogenesis. *Development* **113,** 1193-1206.

Kreidberg, J. A., Donovan, M. J., Goldstein, S. L., Rennke, H., Shepherd, K., Jones, R. C. and Jaenisch, R. (1996). Alpha 3 beta 1 integrin has a crucial role in kidney and lung organogenesis. *Development* **122,** 3537-3547.

Kreidberg, J. A., Sariola, H., Loring, J. M., Maeda, M., Pelletier, J., Housman, D. and Jaenisch, R. (1993). WT-1 is required for early kidney development. *Cell* **74,** 679-691.

Leveen, P., Pekny, M., Gebre-Medhin, S., Swolin, B., Larsson, E. and Betsholtz, C. (1994). Mice deficient for PDGF B show renal, cardiovascular, and hematological abnormalities. *Genes Dev.* **8,** 1875-1887.

Malicki, J., Neuhauss, S. C. F., Schier, A. F., Solnica-Krezel, L., Stemple, D. L., Stainier, D. Y. R., Abdelilah, S., Rangini, Z., Zwartkruis, F. and Driever, W. (1996). Mutations affecting development of the zebrafish retina. *Development* **123,** 263-273.

Marshall, E. K. and Smith, H. W. (1930). The glomerular development of the vertebrate kidney in relation to habitat. *Biol. Bull.* **59,** 135-153.

Miner, J. H. and Sanes, J. R. (1996). Molecular and functional defects in kidneys of mice lacking collagen alpha 3(IV): implications for Alport syndrome. *J. Cell Biol.* **135,** 1403-1413.

Miyamoto, N., Yoshida, M., Kuratani, S., Matsuo, I. and Aizawa, S. (1997). Defects of urogenital development in mice lacking Emx2. *Development* **124,** 1653-1664.

Moore, M. W., Klein, R. D., Farinas, I., Sauer, H., Armanini, M., Phillips, H., Reichardt, L. F., Ryan, A. M., Carver-Moore, K. and Rosenthal, A. (1996). Renal and neuronal abnormalities in mice lacking GDNF. *Nature* **382,** 76-79.

Muller, U., Wang, D., Denda, S., Meneses, J. J., Pedersen, R. A. and Reichardt, L. F. (1997). Integrin alpha8beta1 is critically important for epithelial-mesenchymal interactions during kidney morphogenesis. *Cell* **88,** 603-613.

Newstead, J. D. and Ford, P. (1960). Studies on the development of the kidney of the Pacific Salmon, *Oncorhynchus forbuscha* (Walbaum). 1. The development of the pronephros. *Can. J. Zool.* **36,** 15-21.

Noakes, P. G., Miner, J. H., Gautam, M., Cunningham, J. M., Sanes, J. R. and Merlie, J. P. (1995). The renal glomerulus of mice lacking s-laminin/laminin beta 2: nephrosis despite molecular compensation by laminin beta 1. *Nat. Genet.* **10,** 400-406.

Nussbaum, M. (1886). Ueber den Bau und die Thätigkeit der Drüsen. V. Mittheilung. Zur Kenntnis der Nierenorgane. *Arch.f. mikr. Anat.* **27,** 442.

Oxtoby, E. and Jowett, T. (1993). Cloning of the zebrafish krox-20 gene (krx-20) and its expression during hindbrain development. *Nucleic Acids Res.* **21,** 1087-1095.

Pfeffer, P. L., Gerster, T., Lun, K., Brand, M. and Busslinger, M. (1998). Characterization of three novel members of the zebrafish Pax2/5/8 family: dependency of Pax5 and Pax8 expression on the Pax2.1 (noi) function. *Development* **125,** 3063-3074.

Pichel, J. G., Shen, L., Sheng, H. Z., Granholm, A. C., Drago, J., Grinberg, A., Lee, E. J., Huang, S. P., Saarma, M., Hoffer, B. J., et al. (1996). Defects in enteric innervation and kidney development in mice lacking GDNF. *Nature* **382,** 73-76.

Puschel, A. W., Westerfield, M. and Dressler, G. R. (1992). Comparative analysis of Pax-2 protein distributions during neurulation in mice and zebrafish. *Mech. Dev.* **38,** 197-208.

Sanchez, M. P., Silos-Santiago, I., Frisen, J., He, B., Lira, S. A. and Barbacid, M. (1996). Renal agenesis and the absence of enteric neurons in mice lacking GDNF. *Nature* **382,** 70-73.

Saxén, L. (1987). *Organogenesis of the Kidney.* Cambridge: Cambridge University Press.

Schuchardt, A., D'Agati, V., Larsson-Blomberg, L., Costantini, F. and Pachnis, V. (1994). Defects in the kidney and enteric nervous system of mice lacking the tyrosine kinase receptor Ret [see comments]. *Nature* **367,** 380-383.

Semba, K., Saito-Ueno, R., Takayama, G. and Kondo, M. (1996). cDNA cloning and its pronephros-specific expression of the Wilms' tumor suppressor gene, WT1, from Xenopus laevis. *Gene* **175,** 167-72.

Shawlot, W. and Behringer, R. R. (1995). Requirement for Lim1 in head-organizer function [see comments]. *Nature* **374,** 425-430.

Soriano, P. (1994). Abnormal kidney development and hematological disorders in PDGF beta- receptor mutant mice. *Genes Dev.* **8,** 1888-1896.

Stark, K., Vainio, S., Vassileva, G. and McMahon, A. P. (1994). Epithelial transformation of metanephric mesenchyme in the developing kidney regulated by Wnt-4. *Nature* **372,** 679-683.

Takeyasu, K., Tamkun, M. M., Renaud, K. J. and Fambrough, D. M. (1988). Ouabain-sensitive (Na^+/K^+)-ATPase activity expressed in mouse L cells by transfection with DNA encoding the alpha-subunit of an avian sodium pump. *J. Biol. Chem.* **263,** 4347-4354.

Torra, R., Badenas, C., Darnell, A., Bru, C., Escorsell, A. and Estivill, X. (1997). Autosomal dominant polycystic kidney disease with anticipation and Caroli's disease associated with a PKD1 mutation. Rapid communication. *Kidney Int.* **52,** 33-38.

Torres, M., Gomez-Pardo, E., Dressler, G. R. and Gruss, P. (1995). Pax-2 controls multiple steps of urogenital development. *Development* **121,** 4057-4065.

Toyama, R. and Dawid, I. B. (1997). lim6, a novel LIM homeobox gene in the zebrafish: comparison of its expression pattern with lim1. *Dev. Dyn.* **209,** 406-417.

Tytler, P. (1988). Morphology of the pronephros of the juvenile brown trout, Salmo trutta. *J. Morphol.* **195,** 189-204.

Tytler, P., Ireland, J. and Fitches, E. (1996). A study of the structure and function of the pronephros in the lavvae of the turbot (*Scophthalmus maximus*) and the herring (*Clupea harengus*). *Mar. Fresh. Behav. Physiol.* **28,** 3-18.

Vize, P. D., Jones, E. A. and Pfister, R. (1995). Development of the Xenopus pronephric system. *Dev. Biol.* **171,** 531-540.

Vize, P. D., Seufert, D. W., Carroll, T. J. and Wallingford, J. B. (1997). Model systems for the study of kidney development: use of the pronephros in the analysis of organ induction and patterning. *Dev. Biol.* **188,** 189-204.

Westerfield, M. (1994). *The Zebrafish Book.* Eugene: University of Oregon Press.

Wilson, P. D., Sherwood, A. C., Palla, K., Du, J., Watson, R. and Norman, J. T. (1991). Reversed polarity of Na(+)/K(+)-ATPase: mislocation to apical plasma membranes in polycystic kidney disease epithelia. *Am. J. Physiol.* **260,** F420-430.

Zhou, J., Barker, D. F., Hostikka, S. L., Gregory, M. C., Atkin, C. L. and Tryggvason, K. (1991). Single base mutation in alpha 5(IV) collagen chain gene converting a conserved cysteine to serine in Alport syndrome. *Genomics* **9,** 10-18.